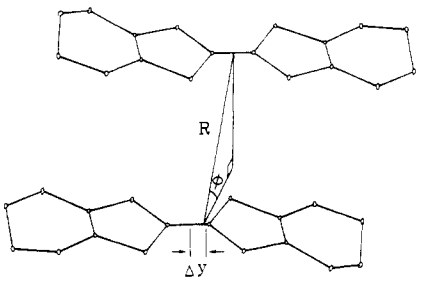

2

have *smaller* interaction energies than (A–F) and (A–G). Among the six possible pairs of interacting ET molecules (see Figure 1), the crystallographically equivalent A–B and A–C pairs have the smallest β_{ij} values, but these pairs contain most of the shortest S···S contact distances. However, the network of S···S distances in the *ab* plane contracts for *all* ET pairs when the IBr_2^- anion replaces the I_3^- anion or when the temperature is reduced (i.e., from 298 to 120 K). As a result of these contracted S···S distances, the intermolecular interactions β_{ij} and the estimated band widths $W_\parallel$ and $W_\perp$ increase systematically.[13]

While the intermolecular S···S distances are important, they are *not* the only measure of the extent of cation–cation interactions. The angle ϕ between the adjacent pair of ET molecules (Table I) is more important on the basis of geometric considerations. Since the HOMO is a π-type orbital, the ϕ values of 0 and 90° represent π- and σ-type interactions, respectively. For intermediate values, partial contributions from either π or σ occur and the net overlap may be positive or negative. The ϕ values for all six ET pairs are compared to the respective β_{ij} values in Table I.

Furthermore, the orbital coefficients of the HOMO of ET, as shown in **3**, reveal that the contribution of S_o is about 3 times smaller than that of S_i.

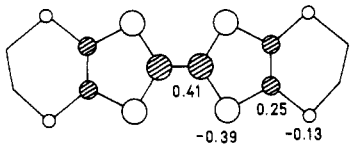

3

Since β_{ij} can be written as

$$\beta_{ij} = \sum_{\mu}\sum_{\nu} C_{\mu i} C_{\nu j} \langle \chi_\mu | H^{\text{eff}} | \chi_\nu \rangle \qquad (1)$$

where $C_{\mu i}$ is the coefficient of the atomic orbital χ_μ in the HOMO ψ_i, the magnitudes of the $S_o\cdots S_o$, $S_i\cdots S_o$, and $S_i\cdots S_i$ interactions have the ratios 1:3:9 in terms of the weighting factors $C_{\mu i}C_{\nu j}$ alone. For these two reasons, the $S_o\cdots S_o$ and $S_i\cdots S_o$ contacts that are less than 3.6 Å do not contribute as significantly to β_{ij} and to the valence band as the $S_i\cdots S_i$ contacts do.

To summarize, the present calculations, which are based on the observed positions of the ET molecules in β-$(ET)_2I_3$ and β-$(ET)_2IBr_2$ obtained from X-ray diffraction experiments, indicate that the intermolecular interactions of the ET molecules *alone* are responsible for the 2D electrical properties. Both the intrastack *and* interstack interactions contribute to the band structure. Our results are consistent with previous findings[17] that the angle ϕ between the adjacent molecular planes of the ET molecules is an important geometric variable in describing the overlap integrals $\langle \psi_i | \psi_j \rangle$ and the interaction energies β_{ij}. While the S···S contacts may be of secondary importance, the $S_i\cdots S_i$ contacts are the most significant among them. The $S_i\cdots S_o$ and $S_o\cdots S_o$ contacts (<3.60 Å) are probably important in terms of crystal packing via core–core interactions and thereby affect the 2D interaction ET network and contribute to the electrical properties of these materials. The systematic comparison of the β_{ij} values in the four crystal structures described here suggests that the substitution of IBr_2^- for I_3^- has the same effect as temperature reduction. Thus, the intermolecular interactions in β-$(ET)_2IBr_2$ at 120 K are the strongest in this series of crystal structures, which suggests that this salt may be a better electrical conductor than β-$(ET)_2I_3$.

Acknowledgment. This work is in part supported by the Camille and Henry Dreyfus foundation through a Teacher-Scholar Award to M.-H.W. Work at Argonne National Laboratory is sponsored by the U.S. Department of Energy, Office of Basic Energy Sciences, Division of Material Sciences, under Contract W-31-109-ENG-38. We express our appreciation for computing time made available by the DOE on the ER-CRAY.

Registry No. β-$(ET)_2I_3$, 89061-05-2; β-$(ET)_2IBr_2$, 92671-95-9.

Supplementary Material Available: Tables of the packing geometries and interaction energies for β-$(ET)_2I_3$ and β-$(ET)_2IBr_2$ at 298 and 120 K (4 pages). Ordering information is given on any current masthead page.

Department of Chemistry
North Carolina State University
Raleigh, North Carolina 27650
Myung-Hwan Whangbo*

Chemistry and Materials Science and Technology Divisions
Argonne National Laboratory
Argonne, Illinois 60439
Jack M. Williams*
Peter C. W. Leung
Mark A. Beno
Thomas J. Emge
Hau H. Wang

Received June 7, 1985

Reaction of Superoxide with Nitric Oxide to Form Peroxonitrite in Alkaline Aqueous Solution

Sir:

Although aqueous superoxide often acts as a one-electron reductant or less frequently as an oxidant, it rarely undergoes covalent bond formation with simple organic or inorganic compounds in water,[1,2] perhaps owing to its poor nucleophilicity in this solvent.[1] In this communication we show, however, that superoxide[3] can react with nitric oxide to form the peroxonitrite anion in deaerated aqueous solutions at pH 12–13:

$$O_2^- + NO = {}^-OONO \qquad (1)$$

This reaction represents one of the few examples[1a] of a radical–radical coupling of O_2^- with another odd-electron species to form a diamagnetic product. The reaction also may be of significance in natural waters[4] or prove useful for trapping and measuring low levels of superoxide in aqueous systems.

Peroxonitrite exhibits a broad absorption spectrum with a maximum at ca. 300 nm. Although stable for hours in 0.1 M base, at lower pH it rapidly protonates and subsequently rearranges to nitrate.[5] $^-OONO/HOONO$ is an intermediate in the reaction of hydrogen peroxide with nitrous acid[6] and in the alkaline autoxidation of hydroxylamine, chloramine, and nitrohydroxamate.[7] Halfpenny and Robinson[6b] reported that NO and H_2O_2 also react to form ^-OONO. However, under the conditions of this study, we found no evidence for this reaction.

Superoxide (15–200 μM) was prepared photochemically in a 1-cm quartz cuvette by the method of McDowell et al.,[8] with use

(1) (a) Sawyer, D. T.; Valentine, J. S. *Acc. Chem. Res.* **1981**, *14*, 393–400. (b) Fee, J. In "Metal Ion Activation of Dioxygen"; Spiro, T. G., Ed.; Wiley-Interscience: New York, 1980; pp 209–237.
(2) (a) Finkelstein, E.; Rosen, G. M.; Rauckman, E. J. *J. Am. Chem. Soc.* **1980**, *102*, 4994–4999. (b) Harbour, J. R.; Chow, V.; Bolton, J. R. *Can. J. Chem.* **1974**, *52*, 3549–3553.
(3) For simplicity, our use of "superoxide" or "$O_2^{-\bullet}$" refers to both O_2^- and its conjugate acid, the hydroperoxyl radical (HO_2), unless otherwise stated.
(4) Zafirious, O. C. In "Chemical Oceanography", 2nd ed.; Academic Press: New York, 1983; Vol. 8, pp 339–379.
(5) Hughes, M. N.; Nicklin, H. G. *J. Chem. Soc. A* **1968**, 450–452.
(6) (a) Gleu, K.; Hubold, R. *Z. Anorg. Chem.* **1935**, *223*, 305. (b) Halfpenny, E.; Robinson, P. L. *J. Chem. Soc.* **1952**, 928–938. (c) Anbar, M.; Taube, H. *J. Am. Chem. Soc.* **1954**, *76*, 6243–6247.
(7) (a) Anbar, M.; Yagil, G. *J. Am. Chem. Soc.* **1962**, *84*, 1790–1796. (b) Yagil, G.; Anbar, M. *J. Inorg. Nucl. Chem.* **1964**, *26*, 453–460 and references contained therein.
(8) McDowell, M. S.; Bakac, A.; Espenson, J. H. *Inorg. Chem.* **1983**, *22*, 847–848.

0020-1669/85/1324-3502$01.50/0

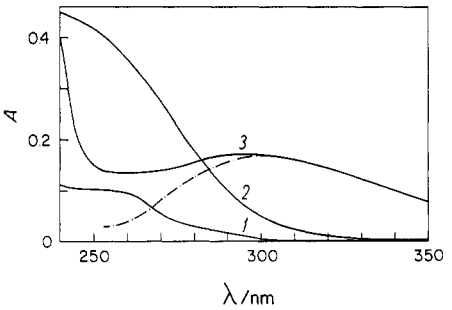

Figure 1. UV absorption spectra: (1) the photochemical system used to generate O_2^-,[8] 5 μM benzophenone (Fluka Chemicals)/5 M 2-propanol (HPLC grade, Fisher Scientific)/100 μM diethylenetriaminepentaacetic acid (Sigma Chemicals) in 0.1 M KOH (O_2 saturated); (2) 135 μM O_2^- solution formed after 20 s of irradiation with a Varian Model 300 UV Xe lamp, followed by deoxygenation with Ar; (3) the product obtained after addition of a 100% excess of NO (270 μM) to the deaerated O_2^- solution. The dashed line (−·−) is a subtraction of spectrum 1 from spectrum 3 below 300 nm. The spectra were recorded on a Cary 15 spectrophotometer modified to allow the deaeration and mixing of a sample directly within the cell compartment (temperature 25 ± 2 °C).

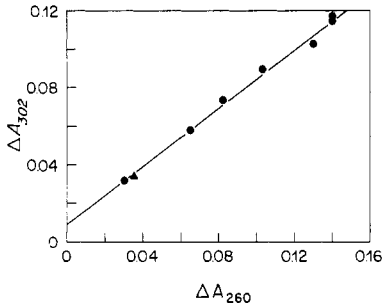

Figure 2. Plot of the absorption increase at 302 nm (ΔA_{302}) vs. the level of O_2^- (absorption at 260 nm, ΔA_{260}) immediately prior to the addition of excess NO.[10] ΔA_{260} and ΔA_{302} were obtained as the difference of spectrum 2 from spectrum 1 and spectrum 3 from spectrum 1, respectively (Figure 1). Differing initial levels of O_2^- were produced by adjusting the time of irradiation and/or the O_2 concentration (air or O_2 saturated) of the photochemical system. The triangle (▲) represents a sample initially 100 μM in O_2^-, which was allowed to decay by dismutation to 20 μM before deaeration and addition of NO.

of 100 μM diethylenetriaminepentaacetic acid instead of EDTA. With this system, the decay of O_2^- exhibited second-order kinetics as assayed spectrophotometrically at 260 nm,[8,9] with the rate constant of dismutation ranging from 2.0 ± 0.2 to 22 ± 3 M^{-1} s^{-1} in 0.1 and 0.005 M KOH, respectively. The slow dismutation rate permitted us to lower the dissolved O_2 concentration to stoichiometrically low levels with respect to O_2^- by rapidly bubbling the irradiated solutions with Ar for ~1 min. This step was undertaken to avoid the reaction of O_2 and NO, which could possibly compete with the O_2^- reaction. A saturated NO_{aq} solution was obtained by bubbling Ar-flushed water (21 ± 2 °C) with 99.9% NO (Matheson). A gastight syringe was used to transfer 100–400 μL of the NO solution to the 1-cm cuvette containing a known volume of the deaerated O_2^- solution. Further details of the procedures are provided in the figure and table legends.

Spectrum 1 of Figure 1 is characteristic of the photochemical sensitizing system; the band at 240–260 nm is due to benzophenone. Irradiation of this solution followed by deaeration produces spectrum 2 (Figure 1), which is a result of O_2^- formation. Within 15 s after addition of a 100% excess of NO over O_2^-, the absorption band due to O_2^- is entirely bleached and a new band with a maximum at ca. 300 nm characteristic of ^-OONO[7b] forms (Figure 1, spectrum 3). The absorption increase at 302 nm (ΔA_{302}) was proportional to the concentration of O_2^- (ΔA_{260}) in the sample immediately prior to injection of excess NO (Figure 2).[10] Assuming the stoichiometry of reaction 1, the slope of Figure 2 represents the ratio of the extinction coefficient of the product at 302 nm to that of O_2^- at 260 nm. This ratio, 0.76, is within 15% of that expected for ^-OONO (0.87) on the basis of the coefficients provided by Bielski[9] for O_2^- (ϵ_{260} = 1925 M^{-1} cm^{-1}) and Hughes and Nicklin[5] for ^-OONO (ϵ_{302} = 1670 M^{-1} cm^{-1}).

Table I. Effect of $[OH^-]$ and $[I^-]$ on the Decay Kinetics of the 300-nm Band[a]

$[OH^-]$, M	$[I^-]$, M[b]	10^5k(obsd), s^{-1}[c]	$[OH^-]$, M	$[I^-]$, M[b]	10^5k(obsd), s^{-1}[c]
0.013		4.7 (4.1)[d]	0.1	0.01	39 (60.6)[f]
0.005		12.7 (6.7)[e]	0.1	0.02	66
0.1	0.005	16 (30)[f]	0.1	0.04	130

[a] The species absorbing at 300 nm was prepared as described in the text and the legend to Figure 1. Three milliliters of this product was subsequently diluted into 17 mL of the appropriate medium within a 10-cm optical cell. The decay was monitored at 302 nm (temperature 25 ± 2 °C). [b] The ionic strength was adjusted to 0.25 with NaCl. [c] Estimated uncertainty ±15%. [d] Value for ^-OONO in 0.01 M KOH from ref 11. [e] Value for ^-OONO in 0.006 M KOH from ref 11. [f] Values for ^-OONO from ref 11.

Addition of equal volumes of the NO solution to unirradiated solutions (deaerated or air saturated) did not produce the 300-nm band, which illustrates that the product cannot result from a reaction of NO with the photochemical system or with O_2. To test whether the product formed via a reaction of NO with H_2O_2, the dismutation (reaction 2) of 100 μM O_2^- was allowed to proceed

$$2O_2^- + 2H^+ = H_2O_2 + O_2 \quad (2)$$

to 80% completion before deaeration and addition of NO. The subsequent increase in absorption at 302 nm was proportional to the residual absorption at 260 nm prior to NO addition (due to the remaining O_2^-; triangle in Figure 2) and not to the amount of the H_2O_2 formed by dismutation. Moreover, the direct addition of 270 μM NO to a deaerated 350 μM solution of H_2O_2 in the same medium did not produce a measurable absorption increase at 302 nm.

The identity of the product as ^-OONO was further corroborated by the decay kinetics of the 300-nm band (Table I). At constant $[OH^-]$, the loss of this band followed first-order kinetics, with the observed rate coefficients varying inversely with OH^- concentration. The coefficients are in good agreement with those measured under comparable conditions by Hughes et al.[11] for ^-OONO decay. Moreover, addition of I^- increased the rate of decay of this absorption band (Table I), in accord with the known reaction of I^- with ^-OONO:[11]

$$^-OONO + I^- + H^+ = NO_2^- + HOI \quad (3)$$

The second-order rate constant for the quenching of the 300-nm band by I^- in 0.1 M KOH, 3.02 × 10^{-2} M^{-1} s^{-1}, is within a factor of 2 of that measured by Hughes et al.[11] for reaction 3.

The results presented here lead to the following two conclusions: (1) O_2^-/HO_2 and NO react to form peroxonitrite in basic aqueous solutions and (2) H_2O_2 and NO do not react to form spectrophotometrically detectable levels of peroxonitrite under these conditions. Our inability to observe formation of ^-OONO from NO and H_2O_2 could result from the exceedingly low yield (≤7%) for this reaction as reported by Petriconi and Papee.[12] Alternatively, the reported NO + HOOH reaction[6b,12] may proceed by complex mechanisms in which intermediates, such as superoxide, are generated by catalytic impurities. By contrast, our results indicate that the reaction of O_2^- with NO to form ^-OONO

(9) Bielski, B. H. J. *Photochem. Photobiol.* **1978**, *28*, 645–649.

(10) Because of the slow decay of O_2^- and the likelihood of a partial loss of NO due to its reaction with residual O_2, a direct titration of an O_2^- solution with NO was not possible. Instead, for a series of samples containing varying levels of O_2^-, a sufficient excess of NO was added to ensure a complete loss of O_2^- and formation of the 300-nm-absorbing product.

(11) Hughes, M. N.; Nicklin, H. G.; Sackrule, W. A. C. *J. Chem. Soc. A* **1971**, 3722–3725.

(12) Petriconi, G. L.; Papee, H. *Can. J. Chem.* **1966**, *44*, 977–980.

occurs in high yield (≥85%, Figure 2) even at micromolar levels of reactants.

The present results do not allow us to distinguish the relative reactivities of O_2^- and HO_2 with NO. Experiments to measure the pH dependence of the kinetics of reaction 1 are in progress. However, a calculation based on the assumptions that (1) HO_2 is the only reactive species and (2) $pK_a(HO_2) = 4.7$ in our reaction medium[13] and on the observation that reaction 1 is complete within 15 s in 0.1 M KOH indicates that the second-order rate constant for the reaction of HO_2 with NO would be above the diffusion-controlled limit. This argues strongly that O_2^- itself reacts with NO at a significant rate.

Acknowledgment. This work has been supported by the Office of Naval Research under ONR Contract N00014-85-C-0001. This is Contribution No. 5968 from the Woods Hole Oceanographic Institution.

Registry No. O_2^-, 11062-77-4; NO, 10102-43-9; ^-OONO, 19059-14-4.

(13) Bielski, B. H. J.; Arudi, R. L. *Anal. Biochem.* **1983**, *133*, 170-178.

Department of Chemistry
Woods Hole Oceanographic Institution
Woods Hole, Massachusetts 02543

Neil V. Blough*
Oliver C. Zafiriou

Received June 24, 1985

Versatility and Low-Temperature Synthetic Potential of Ammonium Halides

Sir:

The obvious successes of the so-called ceramic approach to the synthesis of inorganic solids have led to the conclusion that solid-state *synthesis* is simple and that just brute force, high temperature and/or pressures, and patience have to be applied. However, under such severe reaction conditions, important information on the reaction pathways ("mechanisms"), on intermediates, and on metastable or less stable compounds is almost completely lost. The application of compound or solid-solution precursors[1] has brought considerable improvement in that reaction temperatures are reduced by several hundred degrees because diffusional limitations are overcome by mixing on the atomic scale.

A different approach to the lower temperature synthesis of inorganic solids is the use of highly mobile reagents such as ammonium compounds. We wish to report here the synthetic potential and the versatility of the reactions with ammonium halides, NH_4X (X = Cl, Br, I), as part of a more general program in which ammonium sulfate, nitrate, phosphates, and carbonate are used. The ammonium halides react with rare-earth-metal sesquioxides at temperatures as low as 230 °C (NH_4Cl), 280 °C (NH_4Br), and 360 °C (NH_4I), for example with Y_2O_3 to yield $(NH_4)_3YCl_6$ or with La_2O_3 to yield $(NH_4)_2LaCl_5$.

A variety of different reactants may be applied, not only oxides, but also sulfides, selenides, phosphides, carbides, and the metals themselves. Some of the results are summarized in Table I. The reactants are intimately ground and loaded under dry argon (not mandatory) into Pyrex ampules that have a capillary opening. Optimal reaction temperatures are easily detected by sight when water is one of the products, as it condenses in the capillary, or via the basic reaction of ammonia, which is evolved in many of the reactions, or by reactions of the phosphanes or sulfane with copper sulfate solution. In many cases, the reaction temperature as observed was confirmed by high-temperature X-ray powder patterns (the Guinier-Simon technique[2]) recorded subsequently with the same reaction mixture.

Table I. Survey of the Lower Temperature Syntheses with Binary and Complex Ammonium Halides

reactants	conditions	products
	Redox Reactions	
Li, NH_4Cl	1:2, 270 °C	LiCl, NH_3, H_2
Zn, NH_4Cl	1:4, 270 °C	$(NH_4)_2ZnCl_4$, ...[a]
La, NH_4Cl	1:5, 280 °C	$(NH_4)_2LaCl_5$, ...
Y, NH_4Cl	1:6, 270 °C	$(NH_4)_3YCl_6$, ...
Y, NH_4Br	1:6, 300 °C	$(NH_4)_3YBr_6$, ...
Y, NH_4I	1:6, 390 °C	$(NH_4)_3YI_6$, ...
Cu, NH_4Cl	1:3, 280 °C	$(NH_4)_2CuCl_3$, ...
UH_3, NH_4Cl	1:6, 250 °C	$(NH_4)_2UCl_6$, ...
NH_4ReO_4, NH_4Cl	6:8, 400 °C	Re, N_2, HCl, H_2O
	Acid-Base Reactions	
Li_3N, NH_4Cl	1:3, 250 °C	LiCl, NH_3
$LiYO_2$, NH_4Cl	1:6, 260 °C	$(NH_4)_2LiYCl_6$, NH_3, H_2O
Y_2O_3, NH_4Cl	1:12, 230 °C	$(NH_4)_3YCl_6$, NH_3, H_2O
Y_2S_3, NH_4Cl	1:12, 230 °C	$(NH_4)_3YCl_6$, NH_3, H_2S
YP, NH_4Cl	2:3, 250 °C	$(NH_4)_3YCl_6$, NH_3, PH_3 (P_2H_4)
Y_2O_3, NH_4Br	1:12, 280 °C	$(NH_4)_3YBr_6$, NH_3, H_2O
Y_2O_3, NH_4Br	1:2, 280 °C	YOBr, NH_3, H_2O[b]
Y_2O_3, NH_4I	1:2, 360 °C	YOI, NH_3, H_2O
	Reactions of Complex Ammonium Halides	
$(NH_4)_3YCl_6$, H_2O(g)[c]	350 °C	YOCl, HCl, NH_4Cl
$(NH_4)_3YCl_6$, H_2S(g)	400 °C	YSCl, HCl, NH_4Cl
$(NH_4)_3YCl_6$, Y_2O_3	2:5, 330 °C	YOCl, NH_3, H_2O
$(NH_4)_3YBr_6$, Y_2O_3	2:5, 260 °C	YOBr, NH_3, H_2O
$(NH_4)_3YI_6$, Y_2O_3	2:5, 340 °C	YOI, NH_3, H_2O
$(NH_4)_3YCl_6$, Y_2S_3	2:5, 300 °C	YSCl[d], NH_3, H_2S
$(NH_4)_2EuCl_5$, LiCl	1:2, 280 °C	$(NH_4)_2LiEuCl_6$
	Decompositions	
$(NH_4)_2LiEuCl_6$	350 °C, vac	$LiEuCl_4$, NH_4Cl
$(NH_4)_2UCl_6$	300 °C, vac	UCl_4, ...[e]
$(NH_4)_3YCl_6$	360 °C, GS[f]	$NH_4Y_2Cl_7$, ...
$NH_4Y_2Cl_7$	380 °C, GS	YCl_3, ...
$(NH_4)_3SmBr_6$	365 °C, GS	$(NH_4)_2SmBr_5$, NH_4Br
$(NH_4)_2SmBr_5$	420 °C, GS	$NH_4Sm_2Br_7$, ...
$NH_4Sm_2Br_7$	560 °C, GS	$SmBr_3$, ...

[a] NH_3 and H_2 are evolved, as above. [b] $(NH_4)_3YBr_6$ is produced as an intermediate but reacts promptly with excess Y_2O_3, which is also the case for the reaction of Y_2O_3 with NH_4I (see below). [c] Argon saturated with H_2O vapor at room temperature. [d] Under preparative conditions more or less $NH_4Y_2Cl_7$ is also produced. [e] NH_4Cl is set free, as above. [f] Under the conditions of a temperature-controlled powder pattern study, Guinier-Simon (GS) technique,[2] typical heating rates were 10 °C/h and film speeds were 2 mm/h.

The reactions as summarized in Table I may be divided into two groups, redox and acid-base reactions. In certain cases, NH_4Cl may react as a reductant. For example, when NH_4ReO_4 is heated with NH_4Cl to 400 °C, finely divided Re metal is obtained as the only solid, and N_2, H_2O, and HCl are evolved. Ammonium halides may also react as oxidizing agents with metals, not only the rare-earth metals but also lithium, zinc, and copper, to name only a few. To be specific, it is the H^+ ion that oxidizes the metal. This is interesting because of the relative inertness of copper, but it may be explained by the fact that a stable complex halide, $(NH_4)_2CuCl_3$, is formed simultaneously with the oxidation. Complex formation is also believed to be the driving force of the reactions where, e.g., NH_4Cl reacts as an acid. Again, the H^+ ion is the actual acid and not simply hydrogen chloride that may be formed via the facile dissociation of NH_4Cl.

In either case, NH_4X reacts quantitatively with the appropriate amounts of the reactant used. This has been systematically investigated for the NH_4Cl/Y_2O_3 system: Equimolar amounts within the ranges 2:3 to 12:1 yield $(NH_4)_3YCl_6$ in the first step at 230 °C. When a ratio of 12:1 is used, subsequent decomposition in vacuo around 350 °C yields finely divided, highly active YCl_3, pure on a Guinier basis. The reaction passes through the intermediate $NH_4Y_2Cl_7$. Therefore, the so-called and long known "ammonium chloride route"[3,4] to anhydrous rare-earth-metal

(1) (a) Klemm, W. *Angew. Chem.* **1954**, *66*, 461. (b) Hoppe, R. *Angew. Chem. Int. Ed. Engl.* **1981**, *20*, 63. (c) Horowitz, H. S.; Longo, J. M. *Mater. Res. Bull.* **1978**, *13*, 1359.
(2) Simon, A. *J. Appl. Crystallogr.* **1970**, *3*, 11.

0020-1669/85/1324-3504$01.50/0